

Preparation of a Cu-MOF as an Electrode Modifier for the Determination of Carbendazim in Water

Ya-wei Hu^{1,2,*}, Wei Wang^{1,3}, Huai-en Li¹, Qiang-kun Li² and Ke-ke Niu⁴

¹ Xi'an University of Technology, Xi'an, Shaanxi, 710048, P.R. China

² Yellow River Institute of Hydraulic Research, YRCC, Zhengzhou, Henan, 450003, P.R. China

³ Xiaolangdi Project Construction & Management Center, Ministry of Water Resources, Zhengzhou, Henan, 450004, P. R. China

⁴ Xinxiang Country Agricultural and Pastoral Bureau, Xinxiang, Henan, 453000, P.R. China

*E-mail: huyawei_yrcc@sina.com

Received: 1 February 2018 / Accepted: 10 March 2018 / Published: 10 April 2018

Using a hydrothermal technique, the present study demonstrated the synthesis of a Cu metal–organic framework (Cu-MOF), [Cu(adp)(BIB)(H₂O)]_n (BIB = 1,4-bisimidazolebenzene; H₂adp = adipic acid). Carbendazim was successfully detected by an ultra-sensitive and facile electrochemical sensor fabricated based on the [Cu(adp)(BIB)(H₂O)]_n-coated GCE via differential pulse voltammetry. The present study employed [Fe(CN)₆]^{3-/4-} as an electrochemical probe to investigate the electrochemical properties of our developed sensor. The charge transfer rate and electrode surface of the [Cu(adp)(BIB)(H₂O)]_n/GCE were both more favourable compared to those of the bare GCE. Cyclic voltammetry results suggested a desirable electrochemical performance of our developed sensor towards the detection of carbendazim. Our developed sensor was excellent towards the electrochemical oxidation of the analyte. In addition, the as-prepared electrochemical sensor showed great potential for the detection of carbendazim in water samples.

Keywords: Cu-MOF; Carbendazim; Water sample; Electrochemical determination; [Cu(adp)(BIB)(H₂O)]_n/GCE

1. INTRODUCTION

As a broad-spectrum fungicide, carbendazim (CBZ) has been widely applied in the prevention and control of a variety of diseases that affect vegetables, fruits, and crops [1, 2]. The harmful effects of CBZ on human health have been reported in recent years [3, 4]. In addition, the long persistence of CBZ has also been reported in vegetables, fruits, crops, and the environment [5]. Thus, it is of practical importance to develop a facile, sensitive, and accurate technique for CBZ detection for the benefit of

human health and the environment. Many different analytical strategies, such as chromatography [6-8], spectrophotometry [9-11], and chemiluminescence [12, 13], have been applied towards the determination of CBZ. Additionally, due to their cost effectiveness, short analysis time, easy operation, and favourable sensitivity, electroanalytical strategies have been widely applied in the determination of CBZ. Considering the undesirable response to CBZ using a bare electrode, the electrochemical determination of CBZ has been conducted by modifying a variety of materials, including prominent carbon-based nanomaterials. For the electrochemical oxidation of CBZ, many different carbon nanotube-based electrochemical sensors coated by anionic surfactants [14], mesoporous silica [15], and graphene oxide [16] have been developed. In the present study, CBZ was successfully detected using an improved electrochemical sensor fabricated based on a pyrrolidinium ionic liquid/ordered mesoporous carbon composite system [17]. Considering the exceptional chemical and physical properties, graphene has been widely applied as a potential electrode modifier during the preparation of an electrochemical CBZ sensor [18]. As a kind of carbon-based material electrode, the diamond electrode is another potential analytical tool for the electroanalysis of CBZ [19, 20]. However, electrochemical techniques have been developed for the quantification of CBZ, including heteropolyacid montmorillonite clay-modified electrodes [21], carboxylic group functionalized poly (3,4-ethylenedioxythiophene) mimic electrodes [22], and zeolite-modified electrodes [23].

Metal–organic frameworks (MOFs), with open metal sites, tuneable pore sizes, and high surface areas, show great potential in a variety of fields, such as luminescence, magnetism, sensing, catalysis, and gas storage, thus attracting great research interest [24-27]. MOFs are composed of repeated metal complex units that may be electrochemically activated depending on the ligands and metal ions types. Therefore, MOFs can be developed as electrochemically functional frameworks with favourable electrocatalytic activities and electrochemical features. Many studies have been reported on the oxygen reduction reaction using solid-state Cu-MOFs and Cu-MOF-modified electrodes [28, 29].

In the present study, a novel Cu-MOF, $[\text{Cu}(\text{adp})(\text{BIB})(\text{H}_2\text{O})]_n$ (BIB = 1,4-bisimidazolebenzene; H_2adp = adipic acid) was prepared via a cost-effective, rapid, and facile method. In addition, the preparation can be carried out under benign conditions. The Cu-MOF exhibited a favourable performance towards the electrochemical recognition of the target CBZ under electrochemical conditions.

2. EXPERIMENTS

2.1. Synthesis of $[\text{Cu}(\text{adp})(\text{BIB})(\text{H}_2\text{O})]_n$

Imidazole (5.76 g, 84 mM), 1,4-dibromobenzene (4.72 g, 20 mM), $\text{CuSO}_4 \cdot 5\text{H}_2\text{O}$ (0.064 g, 0.4 mM), and K_2CO_3 (8.78 g, 63 mM) were mixed together and heated for 12 h at 180 °C under an argon atmosphere. After cooling to ambient temperature, the as-prepared mixture was washed with water, and the residue was extracted using 30 mL of reflux ethanol three times. The crude product BIB was produced after the organic layer was separated and evaporated to dryness, followed by its recrystallization in methanol and water.

A mixed solution consisting of BIB (0.4 mM, 84 mg), adipic acid (H_2adp) (0.4 mM, 58 mg), and $CuSO_4 \cdot 5H_2O$ (0.4 mM) was dissolved into 10 ml of distilled water with a 0.5 M solution of NaOH added to adjust the pH to 8.0. Afterwards, the as-prepared mixed solution was sealed in a 25 ml Teflon-lined stainless-steel vessel, followed by heat treatment for 5 days at 160 °C and subsequent slow cooling to ambient temperature. The electrode was made by casting the $[Cu(adp)(BIB)(H_2O)]_n$ on a glassy carbon electrode. The prepared electrode is denoted as $[Cu(adp)(BIB)(H_2O)]_n/GCE$.

Five millilitres of PBS (0.1 M; pH 7.0) with a certain amount of CBZ solution was introduced into the electrochemical cell sealed by a micro-syringe. We immersed the coated electrode in PBS (0.1 M; pH 7.0) containing the desired concentration of CBZ for 90 s under stirring prior to each electrochemical experiment. Differential pulse anodic stripping voltammetry (DPV) was carried out over a range of 0.3 to 1.2 V to investigate the voltammetric determination of CBZ, where the parameters were as follows: amplitude, 0.05 V; potential increase, 0.004 V; pulse interval, 0.2 s; pulse width, 0.05 s. CV was performed at a scan rate range of 10-300 mV/s, and the potential range was 0.1-0.7 V. All test solutions were purged with nitrogen for 10 min to allow for deoxygenation before each measurement.

3. RESULTS AND DISCUSSION

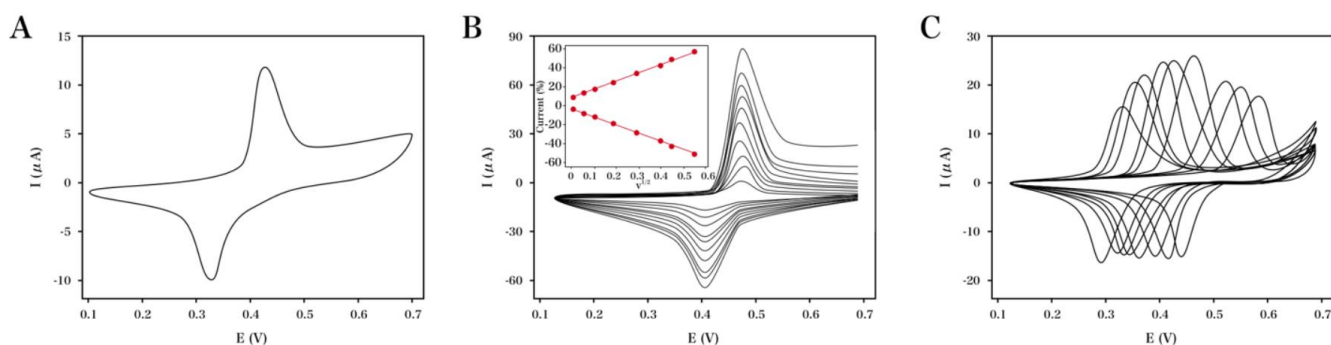


Figure 1. (A) CVs recorded for the $[Cu(adp)(BIB)(H_2O)]_n/GCE$ in a NaOH solution (0.1 M) at a scan rate of 20 mV/s. (B) CVs recorded for the modified electrode in a NaOH solution (0.1 M); scan rates: 0.01, 0.02, 0.04, 0.06, 0.08, 0.10, 0.15, 0.20, 0.25, and 0.30 V/s. Inset: the relationship between the square root of the scan rate and the redox peak current. (C) Solution pH effect on the CV profiles recorded for the modified electrode. (D) Relationship between the pH and the anodic peak potential.

Figure 1A shows the electrochemical performance of the $[Cu(adp)(BIB)(H_2O)]_n/GCE$ in a 0.1 M solution of NaOH; scan rate: 20 mV/s. Two peaks were observed at + 0.39 V (E_{pc}) and + 0.46 V (E_{pa}), as shown in the voltammogram. A linear increase was found between the peak currents and the square root of the scan rate over an increase in the scan rate from 10 mV/s to 300 mV/s (Figure 1B), which implied the diffusion-controlled property of the redox process. Figure 1C illustrates the effect of pH on the electrochemical responses. A negative shift was found for the redox potential as the pH value was increased over a range of 11 to 14.5. The pH showed a linear relationship with the anodic

peak potential (E_{pa}). The slope of 0.061 V/pH was almost equal to the theoretical value of 0.059 V/pH at 25 °C. The electrons acceptance was accompanied by an equal number of hydrogen ions, as suggested by the equation of $-0.061x/n = -0.059$ (x : the number of hydrogen ions participating in the reaction; n : the transferred electron number). Therefore, the reversible oxidation reaction of $[(\text{adp})(\text{BIB})\text{Cu}^{\text{II}}\text{-OH}_2]$ to $[(\text{adp})(\text{BIB})\text{Cu}^{\text{III}}\text{-OH}]$ via a one-proton, one-electron process can be used to describe the electrochemical behaviour of the Cu-MOF in the NaOH solution (0.1 M). The possibility of enhancement resulted from the large surface-to-volume ratio, high electrical conductivity, favourable biocompatibility, excellent catalytic ability and surface reaction activity [30]. Under alkaline conditions, electroneutrality on the surface of electrode can be maintained by the reaction between the H^+ product and the OH^- migrating rapidly from the solution.

The molecular probe in our case was $[\text{Fe}(\text{CN})_6]^{3-/4-}$, whose redox behaviour was studied to investigate the increase in the surface activity of the modified electrode. Figure 2 shows the anodic peak currents for $[\text{Fe}(\text{CN})_6]^{3-}$ (1.0 mM) as a function of the square root of the scan rate. At both electrodes, the square root of the scan rate ($v^{1/2}$) was linearly related to the anodic peak current (i_{pa}). The calculation of the active electrode area was based on the following Randles–Sevcik equation.

$$i_{pa} = 0.446nFA\left(\frac{DnF}{RT}\right)^{1/2}v^{1/2}$$

where n refers to the transferred number of electron(s) during the redox reaction, C refers to the concentration, A refers to the active electrode area, D refers to the diffusion coefficient, and v refers to the scan rate. The other three factors have their conventional meanings ($F = 96,480 \text{ C/mol}$; $T = 298 \text{ K}$, and $R = 8.314 \text{ J mol/K}$). For the bare GCE, the active electrode area was obtained as $0.103 \pm 0.005 \text{ cm}^2$, whilst that of $[\text{Cu}(\text{adp})(\text{BIB})(\text{H}_2\text{O})]_n/\text{GCE}$ was calculated as $0.196 \pm 0.014 \text{ cm}^2$, which implied that the surface modification led to an increased effective surface area of the electrodes, increased electrochemical active sites, an enhanced electrochemical response, which caused the active sites to increase and led to the decrease in the detection limit and enhancement of the electrochemical response [31].

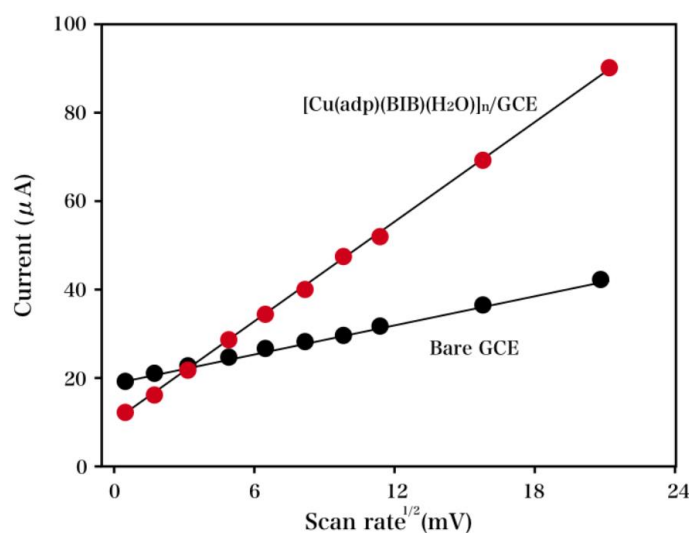


Figure 2. Plots recorded from the bare GCE and $[\text{Cu}(\text{adp})(\text{BIB})(\text{H}_2\text{O})]_n/\text{GCE}$ for the square root of the scan rates versus the anodic peak current of 1 mM $[\text{Fe}(\text{CN})_6]^{3-}$.

The detection performance of the bare GCE and $[\text{Cu}(\text{adp})(\text{BIB})(\text{H}_2\text{O})]_n/\text{GCE}$ towards $5 \mu\text{M}$ CBZ in 0.1 M PBS at $\text{pH } 7.0$ is shown in the CVs of Figure 3A. Over the potential window of $0 - 1.2 \text{ V}$, both electrodes showed a single anodic peak since the CBZ was electrochemically oxidized. The bare electrode exhibited an exceptionally weak anodic peak, whilst single irreversible broad anodic peak currents were obviously enhanced using the $[\text{Cu}(\text{adp})(\text{BIB})(\text{H}_2\text{O})]_n/\text{GCE}$, which suggested that the side chains of $[\text{Cu}(\text{adp})(\text{BIB})(\text{H}_2\text{O})]$ interacted with the target CBZ. Furthermore, this can be attributed to an increase in the thickness of the composite film as the accumulation time lengthened, which would affect the electron transfer rate for metal stripping [32-36].

The electrochemical performance of CBZ was also studied. Figure 3B shows the DPVs recorded for CBZ ($5 \mu\text{M}$) at the bare GCE and $[\text{Cu}(\text{adp})(\text{BIB})(\text{H}_2\text{O})]_n/\text{GCE}$ in 0.1 M of a $\text{pH } 7.0$ PBS. The $[\text{Cu}(\text{adp})(\text{BIB})(\text{H}_2\text{O})]_n/\text{GCE}$ showed a significantly increased anodic peak current towards CBZ than the bare GCE, which displayed a broad and weak anodic peak for CBZ. This comparison indicates the large surface area and favourable conductivity of the former electrode.

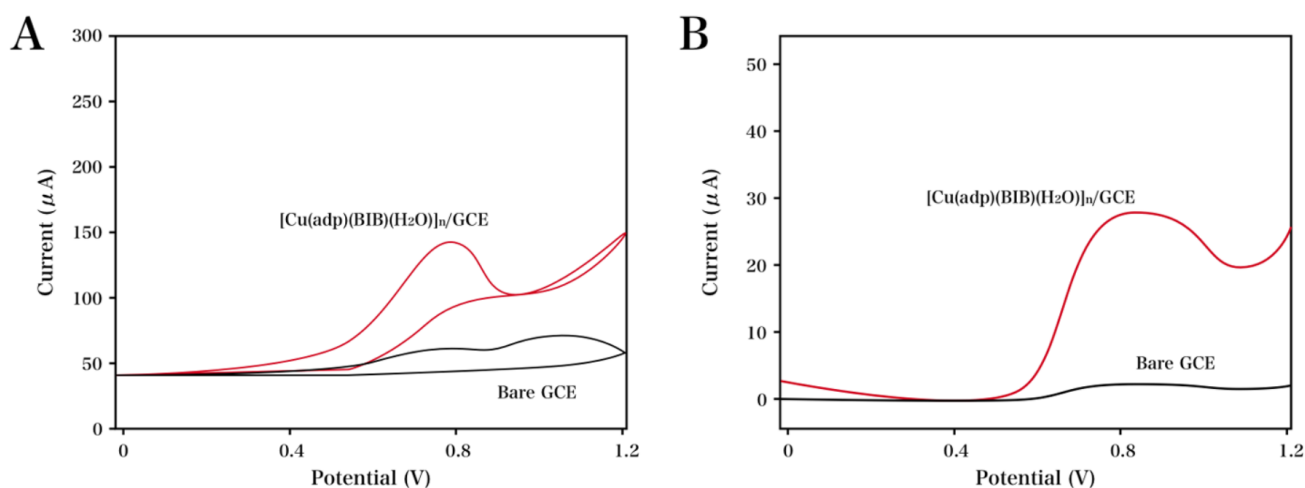


Figure 3. CVs (A) and DPV (B) recorded for CBZ ($5 \mu\text{M}$) at the bare GCE and $[\text{Cu}(\text{adp})(\text{BIB})(\text{H}_2\text{O})]_n/\text{GCE}$ in 0.1 M of a $\text{pH } 7.0$ PBS.

In the present study, we optimized the pH value, accumulation potential, accumulation time, and supporting electrolyte to achieve a more sensitive determination of the target CBZ. Figure 4A presents the influence of the buffer solution pH on the electrochemical response to CBZ. The current response recorded for the analyte CBZ ($5 \mu\text{M}$) as a function of pH ($5.0 - 9.0$) is displayed in Figure 4B. At the $[\text{Cu}(\text{adp})(\text{BIB})(\text{H}_2\text{O})]_n/\text{GCE}$, the anodic peak current of CBZ showed a gradual increase as the pH increased up to a pH of 7.0 ; further increases in the pH led to a sharp decrease in the peak current because CBZ exhibits degradation in basic media. Therefore, the pH was optimized as 7.0 , where the maximal sensitivity could be achieved. Moreover, neutral conditions are also favourable for determination in real environmental conditions [37-39]. Figure 4B also displays the relationship between the pH value and the anodic peak potentials (E_p). The pH increase led to a negative shift in the E_p value, as shown in the equation $E_p \text{ (V)} = -0.052\text{pH} + 1.544$ ($R^2 = 0.99$) based on the formula below:

$$dE_{pa} / dpH = (-2.303mRT) / nF$$

where m refers to the number of protons involved in the electrochemical reaction; n refers to the number of charge transfer during the electrochemical reaction. The m/n ratio using the $[\text{Cu}(\text{adp})(\text{BIB})(\text{H}_2\text{O})]_n/\text{GCE}$ was ~ 1 , which indicates that an equal number of electrons and protons were transferred during the electrochemical reaction of CBZ.

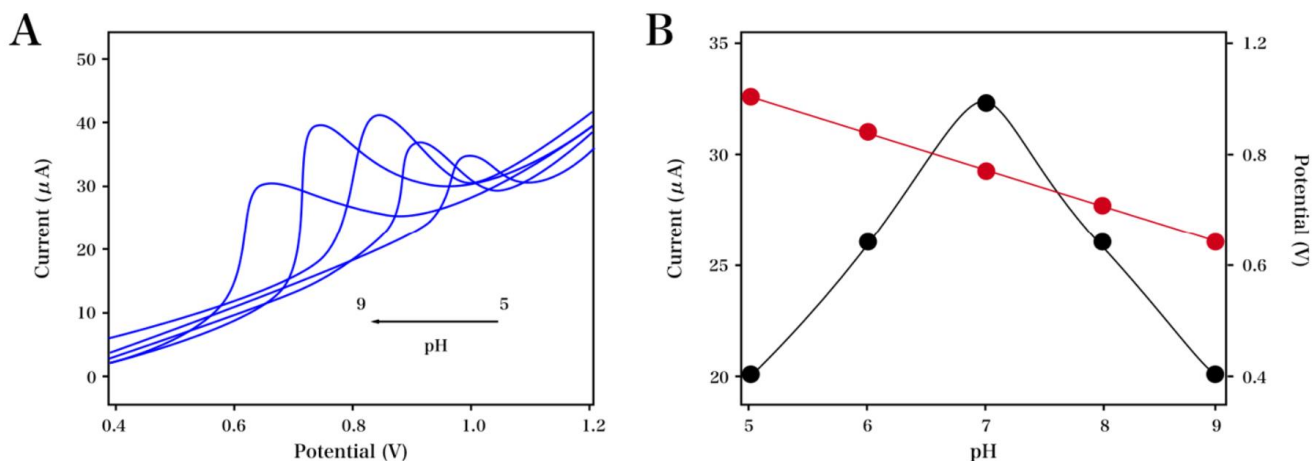


Figure 4. (A) DPV recorded for 5 μM CBZ using the $[\text{Cu}(\text{adp})(\text{BIB})(\text{H}_2\text{O})]_n/\text{GCE}$ at varying pH values; influence of (B) pH value on the anodic peak potentials and the anodic peak currents.

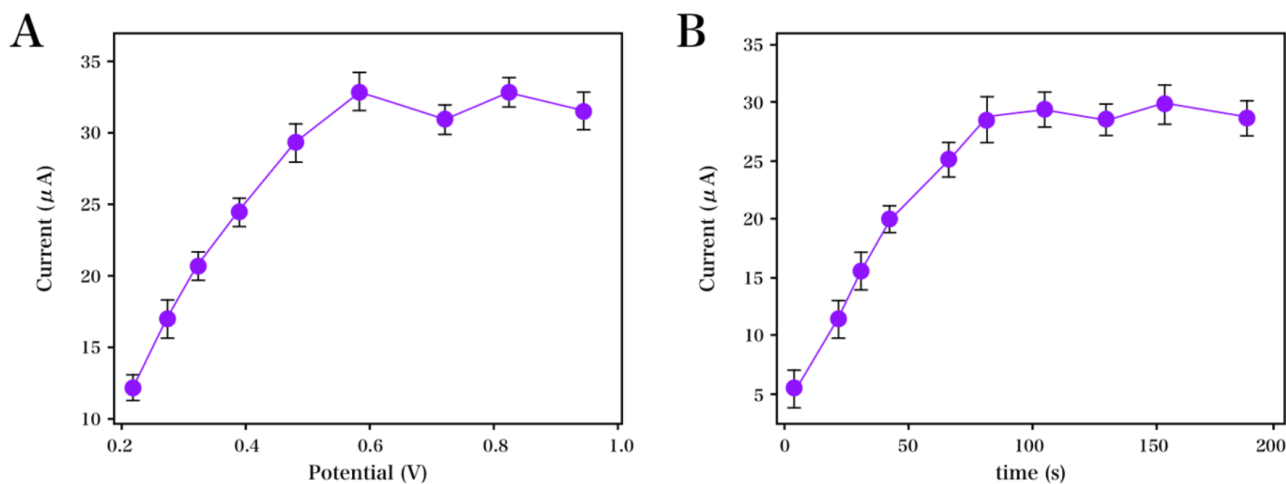


Figure 5. Effect of (A) the accumulation potential and (B) the accumulation time on the current response of 5 μM CBZ in PBS (0.1 M; pH 7.0).

The absorbed amount of CBZ on the electrode surface can be affected by the accumulation parameters, which would further influence the LOD and detection sensitivity. Thus, we studied the accumulation potential and time effects on the detection performance. The effect of the accumulation potential on the current response of 5 μM CBZ in PBS (0.1 M; pH 7.0) is shown in Figure 5A; potential range: 0.2–1.0 V. At a potential of 0.8 V, the anodic peak current reached its maximal value.

Therefore, 0.8 V was selected as the optimum accumulation potential. These phenomena can be attributed to the excellent electrocatalytic activity, high conductivity, large specific surface area of the Cu-MOF [40]. We continued to study the effect of the accumulation time on the anodic current response of the target CBZ by dipping the C-Dots/GCE into CBZ (5 μM) for various accumulation times (Figure 5B). As the accumulation time increased, a sharp increase in the peak current was observed up to 90 s; further increases in time showed no increase in the peak current. Thus, we optimized the accumulation potential and time as 0.8 V and 90 s, respectively.

Due to the on-field detection, low LOD, high selectivity, high sensitivity, favourable simplicity, cost effectiveness, and short time as well as no requirement for pre-treatment or pre-separation, Cu-MOF shows significant potential in electrochemical detection applications. In the presence of CBZ at varying concentrations over a range of 0.1 - 10 μM , DPV responses were recorded using the $[\text{Cu}(\text{adp})(\text{BIB})(\text{H}_2\text{O})]_n/\text{GCE}$ under optimal parameters and are shown in Figure 6. As the CBZ concentration increased to 10 μM , the response current gradually deviated from the linear feature. Less competition for the surface arose as the analyte concentrations decreased, which led to the full coverage of the outermost accessible active surface area. In this case, CBZ uptake would be more efficient, which would result in an improved sensitivity at lower analyte concentrations. Thus, two linear ranges with a change in slope were observed. Over the concentration range of 0.1 to 10 μM , the CBZ concentration was found proportional to the peak current. The limit of quantitation (LOQ) and LOD were obtained as 10 nM and 0.05 μM , respectively, which are both lower than the legally required limits. A comparison of this sensor and other modified sensors towards the detection of CBZ is displayed in Table 1.

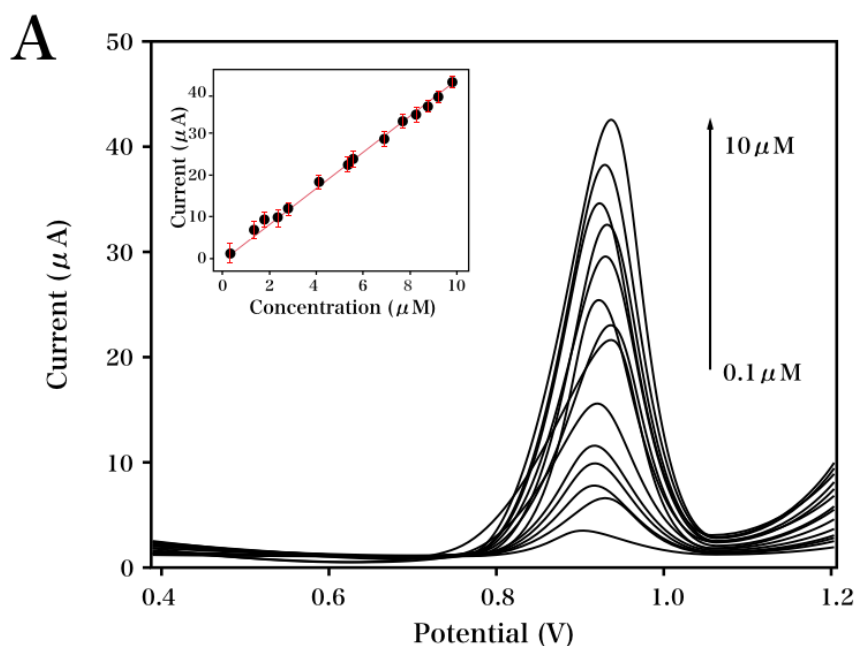


Figure 6. DPVs recorded for CBZ at varying concentrations in PBS (0.1 M; pH 7.0) as the supporting electrolyte using the $[\text{Cu}(\text{adp})(\text{BIB})(\text{H}_2\text{O})]_n/\text{GCE}$ at an accumulation potential of 0.8 V and an accumulation time of 90 s.

Table 1. Comparison of the main properties of the electrochemical sensors towards the determination of CBZ.

Electrode	Linear range upper limit (μM)	Detection limit (nM)	Reference
Sodium montmorillonite clay/GCE	5-100	960	[41]
$\text{SiO}_2/\text{MWCNT}/\text{GCE}$	1-5	56	[15]
MWCNT/GCE	1-10	55	[42]
P-HCNFs/GCE	1-7	38	[43]
$[\text{Cu}(\text{adp})(\text{BIB})(\text{H}_2\text{O})]_n/\text{GCE}$	0.1-10	10	This work

Other measurements of the prepared sensor were performed to identify whether the method was precise and practical. We further studied other performance of the $[\text{Cu}(\text{adp})(\text{BIB})(\text{H}_2\text{O})]_n/\text{GCE}$ to investigate the precision and feasibility of our developed strategy. Twenty consecutive experiments were performed to study the operational stability of our developed sensor towards the electrochemical response of CBZ with a relative standard deviation (RSD) of 2.8%. The result suggested that our developed sensor was highly stable. The long-term stability of the developed sensor towards CBZ ($5 \mu\text{M}$) was studied in 0.1 M of pH 7.0 PBS at an interval of every two days after 1 month of storage in a refrigerator at 4°C . During the initial week, the current response showed no sharp reduction; a further increase in time caused a gradual decrease in the current response. Furthermore, 91.6% of the initial response was retained after 1 month of storage, which suggests that the developed sensor was highly stable over a long period. The oxidation peak current of the target CBZ ($5 \mu\text{M}$) using five as-prepared sensors was compared to study the reproducibility. For five individual detection experiments of CBZ, an RSD of 4.5% was obtained, which suggested that the proposed sensor was highly reproducible. Therefore, the developed sensor was highly stable, as confirmed by its high operation stability, long-term stability, and reproducibility.

Under the optimum parameters, CBZ in tap water was successfully detected using our developed electrochemical sensor via the standard addition method, and the results are compared with the high-performance immunoaffinity chromatography method, as reported [44]. In tap water samples, recoveries were found in a range of 93.2% - 104.1%, as shown in Table 2. This implied the adequacy of our proposed sensor for practical detection even in the absence of sample purification. In addition, the developed sensor was also accurate, efficient, and appropriate for the determination of trace levels of CBZ in real samples.

Table 2. Detection performance of the $[\text{Cu}(\text{adp})(\text{BIB})(\text{H}_2\text{O})]_n/\text{GCE}$ towards CBZ in tap water samples ($n = 5$).

Sample	Added (μM)	Found (μM)	Found by HPIAC (μM)	Recovery (%)
1	0.1	0.095	0.094	95.0
2	0.5	0.467	0.469	93.4
3	1	1.041	1.050	104.1
4	3	3.109	3.141	103.6

4. CONCLUSIONS

Using a hydrothermal technique, the present study proposed the preparation of Cu-MOF from the flexible H₂adp ligand and the rigid BIB ligand. CBZ was successfully detected using the developed [Cu(adp)(BIB)(H₂O)]_n/GCE with a wide linear range of 0.1 to 10 μM and an LOD of 10 nM. Additionally, our developed carbendazim sensor can effectively determine CBZ in environmental tap water samples.

ACKNOWLEDGEMENT

Central public welfare scientific research basic scientific research and special funds: Regional diagnosis model and agricultural non-point source pollution control technology research (HKY - JBYW - 2018-04).

References

1. P.A. Devi, M. Paramasivam and V. Prakasam, *Environmental Monitoring and Assessment*, 187 (2015) 4142.
2. T. Thomidis, T. Michailides and E. Exadaktylou, *Journal of Phytopathology*, 157 (2009) 194.
3. A. Farag, H. Ebrahim, R. ElMazoudy and E. Kadous, *Birth Defects Research Part B: Developmental and Reproductive Toxicology*, 92 (2011) 122.
4. E.M. Rama, S. Bortolan, M.L. Vieira, D.C.C. Gerardin and E.G. Moreira, *Regulatory Toxicology and Pharmacology*, 69 (2014) 476.
5. A. Lewandowska and S. Walorczyk, *Polish Journal of Environmental Studies*, 19 (2010)
6. H. Chen, W. Zhang, Z. Yang, M. Tang, J. Zhang, H. Zhu, P. Lu, D. Hu and K. Zhang, *Instrumentation Science & Technology*, 43 (2015) 511.
7. X. Qin, Y. Xu, Y. Sun, L. Zhao, L. Wang, Y. Sun and X. Liang, *Analytical Letters*, 49 (2016) 1631.
8. Q. Subhani, Z. Huang, Z. Zhu and Y. Zhu, *Talanta*, 116 (2013) 127.
9. M. Chen, Z. Zhao, X. Lan, Y. Chen, L. Zhang, R. Ji and L. Wang, *Measurement*, 73 (2015) 313.
10. N. Pourreza, S. Rastegarzadeh and A. Larki, *Talanta*, 134 (2015) 24.
11. A.D. Strickland and C.A. Batt, *Analytical Chemistry*, 81 (2009) 2895.
12. S. Liao and Z. Xie, *Spectroscopy Letters*, 39 (2006) 473.
13. E. Llorent-Martínez, J. Alcántara-Durán, A. Ruiz-Medina and P. Ortega-Barrales, *Food Analytical Methods*, 6 (2013) 1278.
14. J.M. Petroni, B.G. Lucca, D.K. Fogliato and V.S. Ferreira, *Electroanalysis*, 28 (2016) 1362.
15. C.A. Razzino, L.F. Sgobbi, T.C. Canevari, J. Cancino and S.A. Machado, *Food Chemistry*, 170 (2015) 360.
16. S. Luo, Y. Wu and H. Gou, *Ionics*, 19 (2013) 673.
17. Y. Ya, T. Wang, L. Xie, J. Zhu, L. Tang, D. Ning and F. Yan, *Analytical Methods*, 7 (2015) 1493.
18. P. Noyrod, O. Chailapakul, W. Wonsawat and S. Chuanuwatanakul, *Journal of Electroanalytical Chemistry*, 719 (2014) 54.
19. R.F. Franca, H.P.M. de Oliveira, V.A. Pedrosa and L. Codognoto, *Diamond and Related Materials*, 27 (2012) 54.
20. T. Lima, H. Silva, G. Labuto, F. Simões and L. Codognoto, *Electroanalysis*, 28 (2016) 817.
21. P. Manisankar, G. Selvanathan and C. Vedhi, *Talanta*, 68 (2006) 686.
22. Y. Yao, Y. Wen, L. Zhang, Z. Wang, H. Zhang and J. Xu, *Analytica chimica acta*, 831 (2014) 38.
23. E.M. Maximiano, F. de Lima, C.A.L. Cardoso and G.J. Arruda, *Journal of Applied Electrochemistry*, 46 (2016) 713.
24. Y. Fu, D. Sun, Y. Chen, R. Huang, Z. Ding, X. Fu and Z. Li, *Angewandte Chemie*, 124 (2012)

- 3420.
25. L.T. Nguyen, T.T. Nguyen, K.D. Nguyen and N.T. Phan, *Applied Catalysis A: General*, 425 (2012) 44.
 26. M. Jahan, Q. Bao and K.P. Loh, *Journal of the American Chemical Society*, 134 (2012) 6707.
 27. L.-L. Wen, F. Wang, J. Feng, K.-L. Lv, C.-G. Wang and D.-F. Li, *Crystal Growth and Design*, 9 (2009) 3581.
 28. A. Doménech, H. García, M.T. Doménech-Carbó and F. Llabrés-i-Xamena, *The Journal of Physical Chemistry C*, 111 (2007) 13701.
 29. J. Mao, L. Yang, P. Yu, X. Wei and L. Mao, *Electrochemistry Communications*, 19 (2012) 29.
 30. L. Fu, A. Wang, G. Lai, W. Su, F. Malherbe, J. Yu, C.-T. Lin and A. Yu, *Talanta*, 180 (2018) 248.
 31. L. Zhang, Y. Han, J. Zhu, Y. Zhai and S. Dong, *Anal. Chem.*, 87 (2015) 2033.
 32. H. Li, J. Li, Z. Yang, Q. Xu, C. Hou, J. Peng and X. Hu, *J. Hazard. Mater.*, 191 (2011) 26.
 33. J. Wang, Ü.A. Kirgöz and J. Lu, *Electrochemistry Communications*, 3 (2001) 703.
 34. L. Fu, A. Wang, G. Lai, C.-T. Lin, J. Yu, A. Yu, Z. Liu, K. Xie and W. Su, *Microchim. Acta.*, 185 (2018) 87.
 35. L. Fu, K. Xie, Y. Zheng, L. Zhang and W. Su, *Electronics*, 7 (2018) 15.
 36. L. Fu, K. Xie, H. Zhang, Y. Zheng, W. Su and Z. Liu, *Coatings*, 7 (2017) 232.
 37. J.A. Ribeiro, P.M. Fernandes, C.M. Pereira and F. Silva, *Talanta*, 160 (2016) 653.
 38. L. Chen, X. Zhu, J. Shen and W. Zhang, *Analytical and Bioanalytical Chemistry*, 408 (2016) 4987.
 39. S. Chitravathi and N. Munichandraiah, *Journal of The Electrochemical Society*, 162 (2015) B163.
 40. C.-J. Hsueh, J.H. Wang, L. Dai and C.-C. Liu, *Biosensors*, 1 (2011) 107.
 41. P. Manisankar, G. Selvanathan and C. Vedhi, *Applied clay Science*, 29 (2005) 249.
 42. W.F. Ribeiro, T.M.G. Selva, I.C. Lopes, E.C.S. Coelho, S.G. Lemos, F.C. de Abreu, V.B. do Nascimento and M.C.U. de Araújo, *Analytical Methods*, 3 (2011) 1202.
 43. R. Cui, D. Xu, X. Xie, Y. Yi, Y. Quan, M. Zhou, J. Gong, Z. Han and G. Zhang, *Food Chemistry*, 221 (2017) 457.
 44. D.H. Thomas, V. Lopez-Avila, L. Betowski and J. Van Emon, *Journal of Chromatography A*, 724 (1996) 207